Journal of Geophysical Research: Biogeosciences

RESEARCH ARTICLE
10.1002/2017JG003864

Quantifying the Effects of Snowpack on Soil Thermal and Carbon Dynamics of the Arctic Terrestrial Ecosystems

Zhou Lyu[1] **and Qianlai Zhuang**[1]

[1]Department of Earth, Atmospheric, and Planetary Sciences, Purdue University, West Lafayette, IN, USA

Key Points:
- Snow increased regional winter soils temperature by 6.4°C and influenced land freeze-thaw front northward during 2003-2010
- Snow insulation effects induced 0.41 Pg more C release and shifted Arctic from a C sink to a source of 0.19 PgC/year during 2003-2010
- Model with more detailed snow representation estimated that Arctic will lose 38-51% of permafrost and may transition into a C sink by 2099

Correspondence to:
Q. Zhuang,
qzhuang@purdue.edu

Citation:
Lyu, Z., & Zhuang, Q. (2018). Quantifying the effects of snowpack on soil thermal and carbon dynamics of the Arctic terrestrial ecosystems. *Journal of Geophysical Research: Biogeosciences*, *123*. https://doi.org/10.1002/2017JG003864

Received 31 MAR 2017
Accepted 6 MAR 2018
Accepted article online 25 MAR 2018

Abstract Snow insulation effects modify soil and carbon dynamics in northern middle to high latitudes (45°–90°N). This study incorporates these effects by introducing a snow model into an existing soil thermal model in a biogeochemistry modeling framework, the Terrestrial Ecosystem Model. The coupled model is used to quantify snow insulation effects on carbon and soil thermal dynamics in 45°–90°N region for the historical period (2003–2010) and the future period (2017–2099) under two climate scenarios. The revised model captures the snow insulation effects and improves the estimates of soil thermal dynamics and the land freeze-thaw as well as terrestrial ecosystem carbon dynamics. Historical mean cold-season soil temperature at 5 cm depth driven with satellite-based snow data is 6.4°C warmer in comparison with the original model simulation. Frozen area in late spring is estimated to shrink mainly over eastern Siberia, in central to eastern Europe, and along southern Canada in November. During each nongrowing season in the historical period, 0.41 Pg more soil C is released due to warmer soil temperature estimated using the new model. During 2003–2010, the revised model estimates that the region accumulated 0.86 Pg less C due to weaker gross primary production, leading to a regional C loss at 0.19 PgC/year. The revised model projects that the region will lose 38–51% permafrost area by 2100 and continue to be a C source under the low-emission scenario (Representative Concentration Pathway 2.6) but to be gradually transitioning into a weak sink in the latter half of the 21st century under the high-emission scenario (Representative Concentration Pathway 8.5).

1. Introduction

Rapid climatic changes in the Arctic have been reported over the past decades (Intergovernmental Panel on Climate Change, 2014), with a general decrease in snow cover and frozen season duration, and continual reduction of the Arctic permafrost (Lemke et al., 2007). Spatially, the changes of snow depth in the Arctic vary. While a reduced snow depth was recorded in western North America over the past decades (Bulygina et al., 2009; Dyer & Mote, 2006), there has been an increase in annual snow depth in eastern Siberia (Schindler & Donahue, 2006). This spatial difference in the cryosphere in the past has, not-too-surprisingly, changed the Arctic ecosystem dynamics. Observational studies have shown that there was a stronger atmospheric warming trend in the Arctic than the global mean due to polar amplification resulted from the strong snow-albedo feedback (Serreze & Francis, 2006). Because this feedback is greatly affected by the changes in snow coverage and duration in the Arctic, corresponding changes in air temperature are expected (Déry & Brown, 2007). This will further influence soil temperature. Studies have shown that the warming trend is most likely to continue (McCarthy, 2001) so are the climate-induced changes, including snow cover, permafrost stability, plant growing season length, and plant productivity in boreal and the Arctic ecosystems (Edenhofer et al., 2014, Intergovernmental Panel on Climate Change, 2014). Furthermore, Community Climate System Model has predicted a 10–40% increase in winter snow fall and a shortened snow period (-14 ± 7 days in spring versus $+20 \pm 9$ days in fall) from the 20th to 21st century (Lawrence & Slater, 2010).

Changes in snowpack will alter soil thermal conditions. That largely explained why the magnitude of underground temperature variations in the Arctic does not always directly respond to surface air warming (Lawrence & Slater, 2010). Studies have highlighted the importance of changes in both near-ground air temperature and snow cover on soil thermal regimes in comparison with other factors (Osterkamp, 2007; Osterkamp & Romanovsky, 1999; Stieglitz et al., 2003). A model estimated that more than 50% of the total thermal regime variations in the Arctic can be attributed to snow variability for the latter half of the twentieth century (Lawrence & Slater, 2010). While it can be certain that winter snow cover affects soil temperature, the overall impact on the soil thermal regime depends on the combination of many factors including timing,

duration, density, thickness, and structure of snow as well as local environment (T. Zhang, 2005). To date, the snow insulation effect in the Arctic has not been well quantified using recent satellite-based snow data. Specifically, the existing studies have not explicitly considered the effects of varying snow depth and snow thermal conductivity across space and time.

Further, changing soil temperature, especially in winters, affects ecosystem carbon cycling (Y. Zhang et al., 2008). The Arctic contains a large amount of carbon in plant and soils, which was estimated to be 1,300 PgC with 472 ± 27 PgC in top 1-m soils (Hugelius et al., 2014), accounting for almost half of the global belowground organic carbon (Batjes, 1996; Jobbágy & Jackson, 2000). This large carbon pool is vulnerable to warming soil temperature, which will accelerate carbon mobilization and decomposition processes, leading to more carbon release to the atmosphere. Both long-term records and process-based models confirmed that there has been an increasing carbon release due to soil warming from the 1990s to 2000s (Euskirchen et al., 2017; McGuire et al., 2012). Heterotrophic respiration in nongrowing season is critical to the status of the Arctic soil carbon (Schimel et al., 2006). For instance, studies conducted in boreal European forests and northern Alaska showed that net ecosystem carbon exchanges are largely dependent on the amount of carbon respired during the nongrowing season (Euskirchen et al., 2012; Oechel et al., 2014; Valentini et al., 2000).

Uncertainties in quantifying the carbon budget as the difference between plant productivity and respiration as well as soil decomposition widely exist. For observations, differences in measuring methods and human disturbance often induce uncertainties. For instance, a recent analysis based on observational data at 32 sites in the northern high latitudes found that the Arctic tundra has been a carbon source in the 2000s, with 462 ± 378 TgC released to the atmosphere on an annual basis (Belshe et al., 2013). Another measurement from January 2008 to December 2015 in Alaska indicated a cumulative carbon loss of 158 ± 53 and 668 ± 83 gC/m^2 form heath tundra site and wet sedge tundra site, respectively (Euskirchen et al., 2017). Using on-plot chambers, snow pit chambers, and direct eddy covariance towers, the observed annual CO_2 balance in north Alaskan tundra showed a carbon source from 2009 to 2011, ranging from 22 ± 23 to123 ± 29 gC/m^2/year (Webb et al., 2016). Process-based terrestrial biogeochemical models and atmospheric inversion models also have large uncertainties in their estimates. For instance, two ensemble model simulations spanning over 1990–2006 otherwise suggested that the Arctic tundra is still acting as a carbon sink of 110 and 566 TgC/year, both with large uncertainties between participated models (McGuire et al., 2012, 2016). Retrospective simulations by Hayes et al. (2011) suggested a carbon sink in boreal Europe and Asia but a net source of 27 TgC/year from 1987 to 2006 in boreal North America. Terrestrial biosphere model intercomparison projects on Alaskan Arctic during 2003–2006 with 30 different models estimated that the region acted from a carbon sink to a source of −0.01 ± 0.19 kgC/m^2/year (Fisher et al., 2014).

To constrain the uncertainties of existing estimates of regional carbon budget and more adequately quantify the snow insulation effects on both soil thermal and carbon dynamics, we revised an extant biogeochemistry model, the Terrestrial Ecosystem Model (TEM; Zhuang et al., 2003, 2010). Specifically, a one-dimensional heat transfer snow-soil temperature model was incorporated into the soil thermal model (STM, Zhuang et al., 2001) within TEM. Field measurements of soil temperatures and C fluxes (http://ameriflux.lbl.gov/) were used to calibrate the model. Using this new model, we examined the snow insulation effects on soil temperatures, land freeze-thaw, and C dynamics in the Arctic. This study also took advantage of satellite data of snow cover from AMSR-E/Aqua Level III product (https://nsidc.org/data/docs/daac/nsidc0271_ease_grid_swe_climatology.gd.html, Armstrong et al., 2005), and the recent Arctic permafrost soil C map (http://bolin.su.se/data/ncscd/, Hugelius et al., 2013, 2014). By using the snow depth and snow thermal conductivity derived from the satellite-based snow data, two hypotheses were tested: (1) during the historical period of 2003–2010 land freeze-thaw and soil temperature dynamics as well as subsequent regional terrestrial ecosystem C dynamics are significantly different from the simulations without using these data and (2) the improved snow representation more adequately predicts the permafrost and C dynamics in the Arctic during the 21st century.

2. Methods

2.1. Model Description

In this study, TEM was coupled with an improved STM by including the effects of snow dynamics (Figure 1a). Snow-soil heat exchange was explicitly modeled (Figure 1b). The extant STM was a one-dimensional model

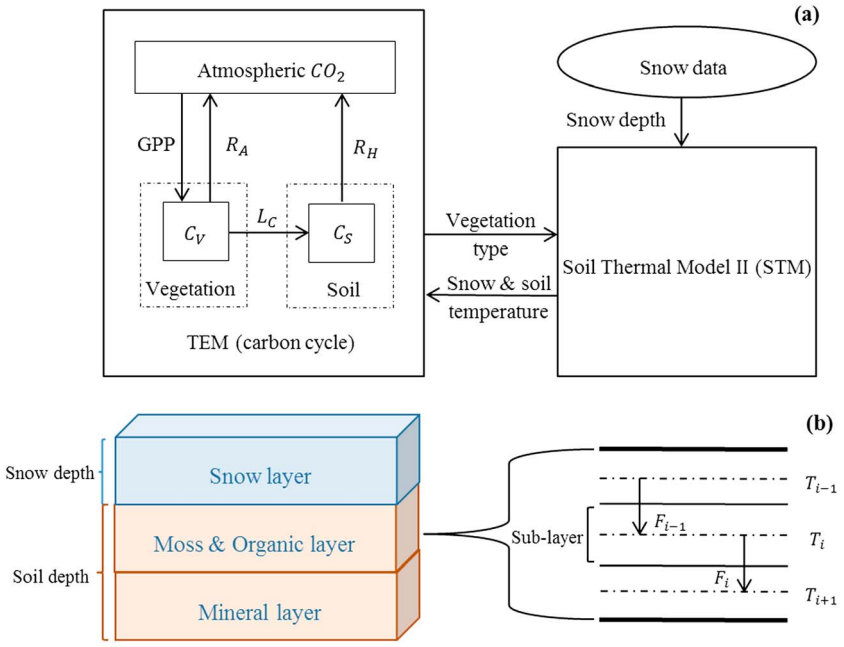

Figure 1. Schematic diagram of the coupled Terrestrial Ecosystem Model (TEM)-Soil Thermal Model (STM), and snow-soil column structure and sublayers in the revised STM.

that models the heat fluxes within soil layers, with consideration of the phase change that accompanies freezing and thawing processes. Soil temperatures were estimated for each depth interval and time step for various soil layers (Zhuang et al., 2001). STM estimated snow layer thickness based on a simple algorithm, and the heat conduction within snow layer has not been explicitly modeled (Zhuang et al., 2001), which introduced discrepancies between observations and simulations when applied on a large spatial scale. This study improved the original model by treating the snow thickness and snow thermal conductivity explicitly in a snow-soil continuum. Snow thickness was estimated from satellite snow water equivalent data, and snow density was calculated based on a snow-classification system of Sturm et al. (1995, 2010). The simulated temperature at the snowpack bottom was used for the upper boundary condition of the soil profile. Previous research has indicated that the temperature profile within the snowpack generally follows a linear pattern (Cherkauer & Lettenmaier, 1999), which was employed in this study. STM-TEM was run to equilibrium, so the heat flux at the snow-soil interface from the snow side equals the ground heat flux at the soil-snow interface coming from the soil column, calculated from the existing STM. The upper boundary condition of the upper snow surface temperature equals the near-ground air temperature, while the lower boundary condition at the snow-soil interface was allowed to change as follows:

$$K_{\text{snow}} \frac{\Delta T_{\text{snow}}}{\Delta Z_{\text{snow}}} = G = -K_{\text{soil}} \frac{\Delta T_{\text{soil}}}{\Delta Z_{\text{soil}}} \tag{1}$$

where K_{snow} is the snow thermal conductivity (W/m/K), and K_{soil} is the soil thermal conductivity (W/m/K). ΔZ_{snow} (m) was the snow depth, and ΔZ_{soil} (m) is the simulated soil column depth. ΔT_{snow} (°C) is the temperature change through the snowpack from snow surface (where the temperature was defined as air temperature) to the bottom of snowpack, and ΔT_{soil} (°C) in this particular module is the temperature change through the STM-simulated soil column. Temperature at the bottom of snowpack was assumed to be the same as temperature at the soil surface; thus, equation (1) can be expanded as follows:

$$T_{\text{snowbase}} = \frac{T_{\text{air}} + \frac{K_{\text{soil}}}{K_{\text{snow}} \cdot \Delta Z_{\text{soil}}} \cdot \Delta Z_{\text{snow}} \cdot T_{\text{soilbase}}}{1 + \frac{K_{\text{soil}}}{K_{\text{snow}} \cdot \Delta Z_{\text{soil}}} \cdot \Delta Z_{\text{snow}}} \tag{2}$$

Air temperature at current time step and calculated soil temperature profile from the previous time step were substituted into equation (2) to solve for the initial snowpack bottom temperature at this time step, which was then fed back to STM as the upper boundary condition for an intermediate soil temperature profile.

These calculations were iterated multiple times in order to balance the monthly heat flux at the interface between snow and soil. The temperature at the snowpack bottom from the final iteration was taken as the upper boundary condition to solve for the final soil temperature profile for the current time step. In contrast, the previous version of STM simply used air temperature as the upper boundary condition (Zhuang et al., 2001).

The snow thermal conductivity used in equation (2) was approximated from its density, following the empirical relationship summarized by Sturm et al. (1997). The snow depth Z_{snow} in the heat flux equation was calculated from the snow water equivalent data, obtained from the satellite data product (Armstrong et al., 2005). Each ecosystem type had a prescribed constant bulk snow density. This density was estimated for the whole snow layer without distinguishing the density differences between fresh and old snow within a month. A minimum acceptable snow thickness of 0.01 m was set in the model.

TEM was a process-based biogeochemical model that quantifies the net ecosystem production (NEP), the difference between gross primary production (GPP), the autotrophic respiration (R_A) that included both growth and maintenance respiration of living vegetation, and the heterotrophic respiration (R_H) that represented soil decomposition. GPP, the amount of chemical energy synthesized as biomass in an ecosystem, was calculated as (Zhuang et al., 2003)

$$\mathrm{GPP} = C_{\max} f(\mathrm{PAR}) f(\mathrm{LEAF}) f(T) f(C_a, G_V) f(\mathrm{NA}) f(\mathrm{FT}) \tag{3}$$

where C_{max} is the maximum rate of C assimilation, PAR is photosynthetically active radiation, LEAF is the leaf area relative to the maximum annual leaf area, T is temperature in °C, C_a is atmospheric carbon dioxide content, G_V is the relative canopy conductance, and NA is nitrogen availability. f(NA) is defined as the feedback of nitrogen availability on the carbon assimilation. f(FT) reflects the influence of freeze-thaw on vegetation CO_2 uptake.

In TEM, soil respiration is represented by R_H, which is calculated as follows:

$$R_H = K_d C_s f(M_V) e^{0.0693\mathrm{T}} \tag{4}$$

where K_d is the heterotrophic respiration rate at 0°C, C_s is carbon storage in soils, and T is the monthly mean soil temperature at top 20 cm depth that influenced respiration (the exponential form of T on R_H reproduces the temperature sensitivity of soil decomposition). $f(M_V)$ is a nonlinear relationship that defines the influence of volumetric soil moisture (M_V) on soil decomposition (Tian et al., 1999):

$$f(M_V) = \frac{(M_V - M_{V\min})(M_V - M_{V\max})}{(M_V - M_{V\min})(M_V - M_{V\max}) - (M_V - M_{V\mathrm{opt}})^2} \tag{5}$$

where $M_{V\min}$ (0%), $M_{V\mathrm{opt}}$ (50%), and $M_{V\max}$ (100%) are the minimum, optimum, and maximum volumetric soil moisture content considered for soil respiration. When soil temperature is below −1°C, $f(M_V)$ is assumed with a very small value of 0.001.

The extant TEM has been well parameterized and calibrated to various ecosystem types (Zhuang et al., 2003).

2.2. Data Sets

Monthly climate data for the period of 2003–2010 including air temperature (°C), precipitation (mm), and radiation (W/m^2) obtained from Climate Research Unit database (Mitchell et al., 2004) were used to run historical simulations. Aside from these time series data, gridded global-scale soil texture data were organized based on the Food and Agriculture Organization (1974) soil map of the world. The input vegetation map was obtained from Melillo et al. (1993), and the elevation values for the whole study region were obtained from 10-min digital global elevation data (NCAR/NAVY, 1984). Global Monthly EASE-Grid Snow Water Equivalent (SWE) data derived from the AMSR-E instrument carried on the NASA Earth Observing System Aqua satellite (https://nsidc.org/data/docs/daac/nsidc0271_ease_grid_swe_climatology.gd.html, Armstrong et al., 2005) were used for the revised model. This data set has been evaluated for a list of chosen areas in northern high latitudes. For instance, satellite-based SWE was well close to observations for Canadian high plains and Russian steppe area with R^2 between 0.75 and 0.8. The accuracy for mountainous and heavily forested areas was less with R^2 around 0.5 (Armstrong & Brodzik, 2002; Armstrong et al., 2005; Chang et al., 1987).

Table 1
Description of Calibration Sites

Site name	Location	Calibrated soil layer thickness (cm)	Ecosystem type	Vegetation cover	Soil type	Annual mean temperature (°C)	Annual precipitation (mm)	Reference
Imnavait US-ICt	68.6°N, 149.3°W	22	Alpine tundra	Sedge, shrubs	Permafrost	−7.4	318	Ueyama et al. (2013)
Barrow US-Brw	71.3°N, 156.6°W	20	Wet tundra	Sedge, shrubs	Permafrost	−12.6	85 (summer)	Ikawa and Oechel (2014) and Kwon et al. (2006)
BOREAS NSA old black spruce	55.9°N, 98.5°W	20	Boreal forest	Black spruce	Kame and clay soil	−3.2	517	McCaughey et al. (1997) and Bond-Lamberty et al. (2005)
Sylvania Wilderness US-Syv	46.2°N, 89.3°W	20	Coniferous forest	Hemlock-hardwood	Spodosol	3.81	826	Desai et al. (2005)
Ivotuk US-Ivo	68.4°N, 155.7°W	22	Alpine tundra	Tussock, shrubs	Permafrost	−10.9	202	Riedel et al. (2005)
Atqasuk US-Atq	70.5°N, 157.4°W	20	Wet tundra	Sedge	Sandy, permafrost	−11.9	55 (summer)	Oberbauer et al. (2007)
Howland Forest/ US-Ho1	45.2°N, 68.7°W	20	Coniferous forest	Spruce, hemlock	Glacial tills	6.2	1148	Hollinger et al. (1999)

Using site-level measurements from the standardized AmeriFlux data set (http://ameriflux.lbl.gov/), carbon dynamics were calibrated. The calibration site description was documented in Table 1, and the comparison between modeled and observed carbon fluxes has R^2 from 0.71 to 0.83 (Figure 2).

Soil thermal parameters were calibrated at several sites (Table 1). At each site, a set of climate and soil thermal data were obtained from the standardized AmeriFlux data set (http://ameriflux.lbl.gov/). The representative sites include the following: Imnavait Alaska site for the alpine tundra ecosystem (Ueyama et al., 2013), Barrow Alaska site for wet tundra-type land cover (Zona et al., 2016), BOREAS NSA old black spruce forest Canada site for boreal forest type (McCaughey et al., 1997), and North Sylvania Wilderness Michigan site for coniferous forest type (Desai et al., 2005).

2.3. Model Parameterization and Regional Simulation

The revised STM was parameterized using site measurement at various depths. The model estimates can be expressed as follows:

$$\widehat{Y} = f(X|\theta) + \mathrm{e} \tag{6}$$

where $\widehat{Y} = (y_1, y_2, \cdots, y_n)$ is the model outputs vector containing time series of soil temperatures. f is the simplified expression of the simulation process functions built within the TEM. X is the input data that drives the model. $\theta = (\theta_1, \theta_2, \cdots, \theta_m)$ is the vector of a set of m unknown parameters to be calibrated. $e = [e(\theta_1), e(\theta_2), \cdots e(\theta_m)]$ are independently and identically distributed errors of the simulation.

The goal of parameterization here was to identify the topsoil layer parameter set that minimized the statistical error e by generating thousands of parameter sets for the model using Latin hypercube sampling method (Iman, 2008). To ensure the reliability of the parameterization and calibration results, the parameters sample size was set to be 10,000. It should be noted that soil thermal parameters are not uniform throughout the soil profile. In this study, only the parameters of the top organic soil layer were calibrated for several reasons. First, the topsoil layer is where main microbial activity takes place due to its rich C and abundant microbes (Fierer et al., 2003; Fisk et al., 2003; Taylor et al., 2002). Second, the topsoil layer is strongly affected by snow insulation effects and air temperatures (Brady & Weil, 2013). Third, in situ measurements of soil temperature are mostly down to soil depth of 20 cm. Finally, the parameters for deep soil layers have been calibrated in our previous studies (Zhuang et al., 2001, 2003). The prior ranges and optimized values of the calibrated topsoil layer parameters in this study were ecosystem type specific (Table 2).

Two sets of model simulations were conducted for the historical period of 2003–2010: (1) the simulations with the previous version of TEM (TEM_S1 model), not considering the thermal effects of changing snow cover and (2) the simulations with the revised STM-TEM (TEM_S2 model) that used satellite-derived snow water equivalent data. TEM_S2 simulations were driven with AMSR-E SWE data, in addition to the climate forcing data used in TEM_S1. To predict future ecosystem C fluxes and soil C changes, the revised model was run

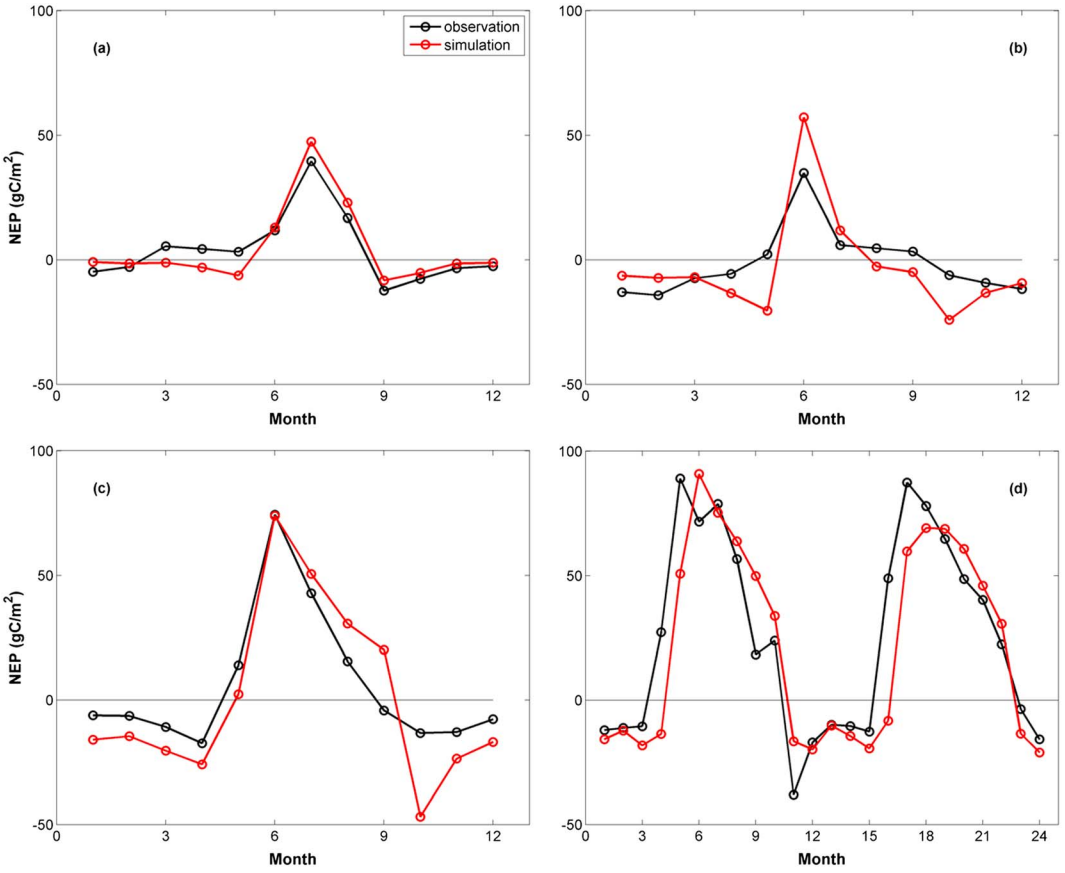

Figure 2. Simulated and observed net ecosystem production fluxes at (a) Ivotuk for alpine tundra, (b) Atqasuk for wet tundra, (c) BOREAS for boreal forest, and (d) Howland forest for coniferous forest.

from 2017 to the end of 2099, driven by two future climate scenarios Representative Concentration Pathways, RCP 2.6 and RCP8.5 from the general circulation model Hadley Centre Global Environmental Model, version 2 (Baek et al., 2013; Martin et al., 2011) developed by the Met Office Hadley Centre in UK. The climate and atmospheric CO_2 data were obtained from the World Climate Research Programme's Coupled Model Intercomparison Project phase 5 multimodel data set (https://esgf-node.llnl.gov/projects/cmip5/, Taylor et al., 2012). Gridded soil carbon stock data from the Arctic permafrost soil C map (http://bolin.su.se/data/ncscd/) produced by Hugelius et al. (2013, 2014) were used as initial soil C for each grid for all model simulations. Total soil organic C in this data set has been quantified with an uncertainty range of ±15% (Hugelius et al., 2014).

Additional simulations were conducted to examine the uncertainties of snow insulation parameters of the snow thermal conductivity K_{snow} and soil thermal conductivity (K_{soil}), in affecting winter thermal dynamics and their effects on C dynamics. Specifically, for each ecosystem type, three simulations were conducted, including a baseline simulation that used the calibrated snow thermal conductivity and two other simulations by varying the calibrated snow conductivity by ±25%. Similarly, for each ecosystem type, three simulations were conducted to examine the effects of changing soil thermal conductivity.

3. Results and Discussion

3.1. Model Verification

The revised STM-TEM well reproduced the observed soil temperature at topsoil layers for alpine tundra, wet tundra, boreal forest, and coniferous forest ecosystem types, especially over the cold seasons (Table 3 and Figure 3). The revised performed better than the original model. The uncertainty analysis by varying snow and soil thermal conductivity showed a similar sensitivity in affecting winter thermal and C dynamics.

Table 2
Prior Range and Optimized Soil Parameter Values in Soil Thermal Model

Parameter description	Alpine tundra	Wet tundra	Boreal forest	Coniferous forest
Prior water content (%)	[0.1, 0.8]	[0.1, 0.8]	[0.1, 0.8]	[0.1, 0.8]
Optimized water content (%)	0.365	0.829	0.568	0.501
Prior frozen soil thermal conductivity (Wm^{-1} K^{-1})	[0.01, 4]	[0.01, 4]	[0.01, 4]	[0.01, 4]
Optimized frozen soil thermal conductivity (Wm^{-1} K^{-1})	1.4	3.126	2.620	1.027
Prior thawing soil thermal conductivity (Wm^{-1} K^{-1})	[0.01, 4]	[0.01, 4]	[0.01, 4]	[0.01, 4]
Optimized thawing soil thermal conductivity ($Wm^{-1}K^{-1}$)	0.049	0.603	0.742	0.887
Prior frozen soil heat capacity (KJm^{-3} K^{-1})	[300, 3,500]	[300, 3,500]	[300, 3,500]	[300, 3,500]
Optimized frozen soil heat capacity (KJm^{-3} K^{-1})	3191.4	2995.2	2,520.0	2,888.5
Prior thawing soil heat capacity (KJm^{-3} K^{-1})	[300, 3,500]	[300, 3,500]	[300, 3,500]	[300, 3,500]
Optimized thawing soil heat capacity (KJm^{-3} K^{-1})	2,060.5	1,906.8	1,431.5	999.0

Across different ecosystem types, snow bottom temperatures from the test simulations differed between −18.6% and 22.1% from the simulated baseline temperature. Differences in R_H and NEP estimated from test simulations were between −7.6% and 13.1% for R_H, and between −7.2% and 11.8% for NEP, respectively (Table 4).

Snow insulation effects enhanced winter soil respiration. Our revised estimates of the total cold-season respiration fell well within the range of previous field studies in boreal and tundra ecosystems. For instance, total cold season CO_2 emissions at Adventdalen, Svalbard, (near 78°N, 16°E) from October 2007 to May 2008 were estimated to be 41.8 gCO_2/m^2/year with the revised model, which was close to the diffusive flux chamber measurement of 53 ± 18 gCO_2/m^2/year at this Arctic tundra site spanning from 2 October 2007 to 29 May 2008 (Björkman et al., 2010). Soda lime chamber CO_2 flux measurements at a Canadian mixed tundra site (Tundra Ecological Research Station at Daring Lake, Northwest Territories, Canada, near 65°N, 111.5°W) with both dry heath and wet sedge vegetation types reported total cold season respiration between 34 and 126 gCO_2-C/m^2/year over 294 days from the end of August 2006 to mid-June 2007 (Grogan, 2012). In comparison, our model estimation of 114.4 gC/m^2/year during the period was well at the high end of their measurements. A recent eddy covariance study for northern Alaska alpine tundra (Imnavait Creek, near 68.5°N, 149.5°W) estimated cold-season net ecosystem exchanges of 121, 72, and 105 gCO_2-C/m^2/year (cold season respiration of 118, 67, and 98 gCO_2-C/m^2/year) for the three consecutive cold seasons between 2007 and 2010 (Euskirchen et al., 2012), which were comparable to our NEP estimates of 104.9, 103.8, and 104.5 gCO_2-C/m^2/year (soil respiration of 102.3, 101.9, and 103.0 gCO_2-C/m^2/year) over the same period, respectively. Site-level comparisons between simulated and observed NEP showed that the revised model better captured annual C fluxes with R^2 of 0.79 at Ivotuk alpine tundra site during the cold season in 2006, 0.75 at Ataqsuk wet tundra site from 2003 to 2004, 0.80 at BOREAS boreal forest site in 2003, and 0.74 at Howland coniferous forest site from 2003 to 2004, respectively.

3.2. Soil Thermal Dynamics

Soil temperature estimation at 5-cm depth in the snow-free summer months from both models was close (less than 0.05°C difference) over the entire study area, while soil temperatures in cold season (from October to the next May, Figure 4) had noticeable differences due to snow. Soil cooled slower from October to November and also warmed slower from April to May, comparing to the original estimation (Figure 4). Earlier warm winter soil conditions allowed longer transition before soils frozen, affecting winter soil thermal conditions. Mean soil temperatures at 5 cm depth from November to the following March in the revised estimations were approximately 6.4°C warmer than that of the original model (Figure 4). This increase of soil temperature corresponded well to the observed snow insulation effects on ground thermal conditions from a previous snow manipulation experiment in a mixed boreal forest in New Hampshire (Hardy et al., 2001). Snow insulation affected the soil column as a whole, increasing temperatures of the soil column from surface downward. The insulation effect weakens

Table 3
Site-Level Topsoil Temperature Calibration Statistics for the Revised Model for Major Ecosystem Types

Site	Ecosystem type	RMSE (°C)	R^2	Slope
Imnavait	Alpine tundra	2.16	0.84	1.76
Barrow	Wet tundra	2.76	0.79.	0.93
Boreas	Boreal forest	2.49	0.73	0.94
Sylvania	Coniferous forest	2.06	0.93	0.93

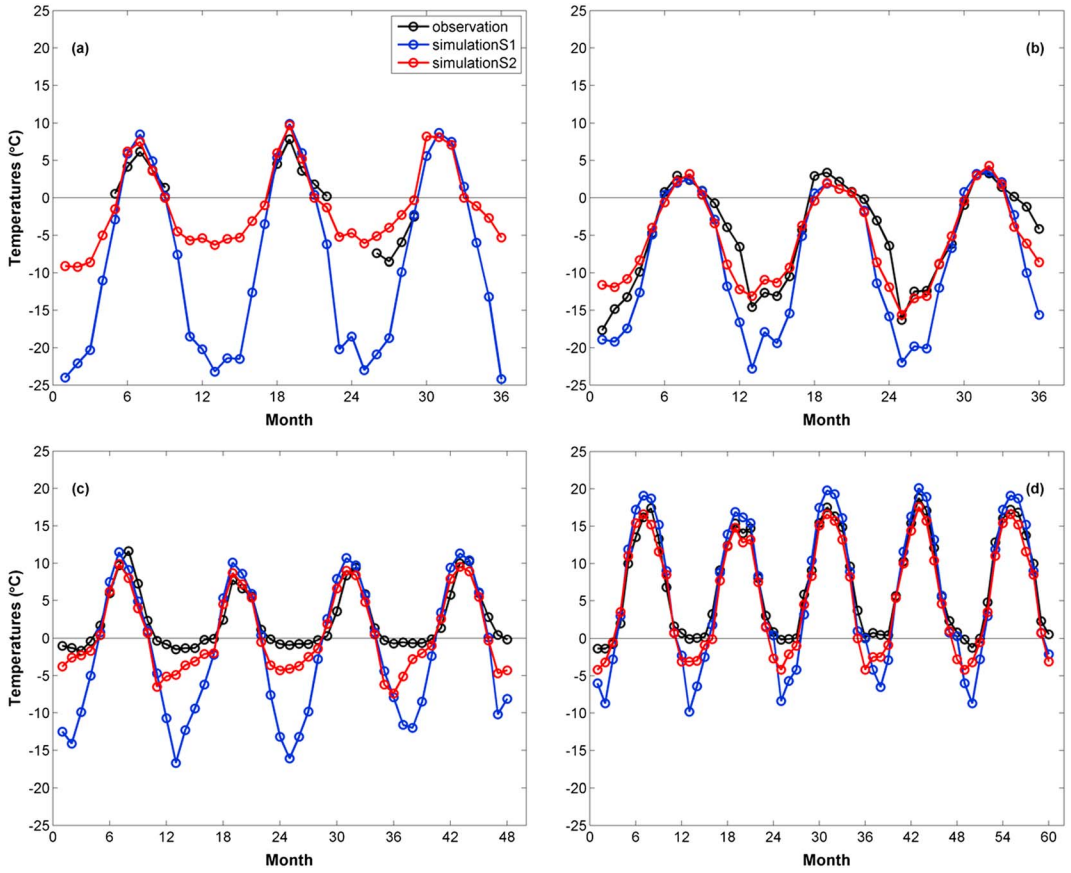

Figure 3. Simulated and observed 5-cm soil temperatures from two versions of the model at (a) Imnavait for alpine tundra, (b) Barrow for wet tundra, (c) BOREAS for boreal forest, and (d) Sylvania wilderness for coniferous forest.

Table 4
Uncertainty of the Revised Model (S2) in Winter Snow Bottom Temperature ($T_{snowbott}$), R_H, and NEP, in Response to Varying Conductivity Parameters of K_{snow} and K_{soil}, Respectively

Ecosystem type	ΔK_{snow}	ΔK_{soil}	$T_{snowbott_{baseline}}$ (°C)	$\Delta T_{snowbott}$	$R_{Hbaseline}$ (gC/m^2)	ΔR_H	$NEP_{baseline}$ (gC/m^2)	ΔNEP
Alpine tundra	+25%	—	−9.7	+15.79%	1.68	−4.76%	−1.7	−5.88%
	−25%	—		−18.56%		+13.10%		+11.76%
	—	+25%		−16.49%		+7.14%		+5.88%
	—	−25%		+19.59%		−4.79%		−5.90%
Wet tundra	+25%	—	−18.1	+8.29%	19.1	−5.76%	−19.2	−5.24%
	−25%	—		−11.60%		+7.85%		+7.85%
	—	+25%		−9.39%		+3.66%		+3.64%
	—	−25%		−10.50%		−3.14%		−3.14%
Boreal forest	+25%	—	−6.8	+16.18%	23	−5.65%	−23.5	−5.11%
	−25%	—		−17.65%		+6.52%		+6.81%
	—	+25%		−14.71%		+5.22%		+5.53%
	—	−25%		+22.06%		−7.56%		−7.23%
Coniferous forest	+25%	—	−5.8	+12.07%	7.9	−2.53%	−10.6	−2.83%
	−25%	—		−13.79%		+5.06%		+2.83%
	—	+25%		−12.06%		+3.80%		+1.89%
	—	−25%		+15.52%		−3.79%		−2.82%

Note. R_H = heterotrophic respiration; NEP = net ecosystem production.

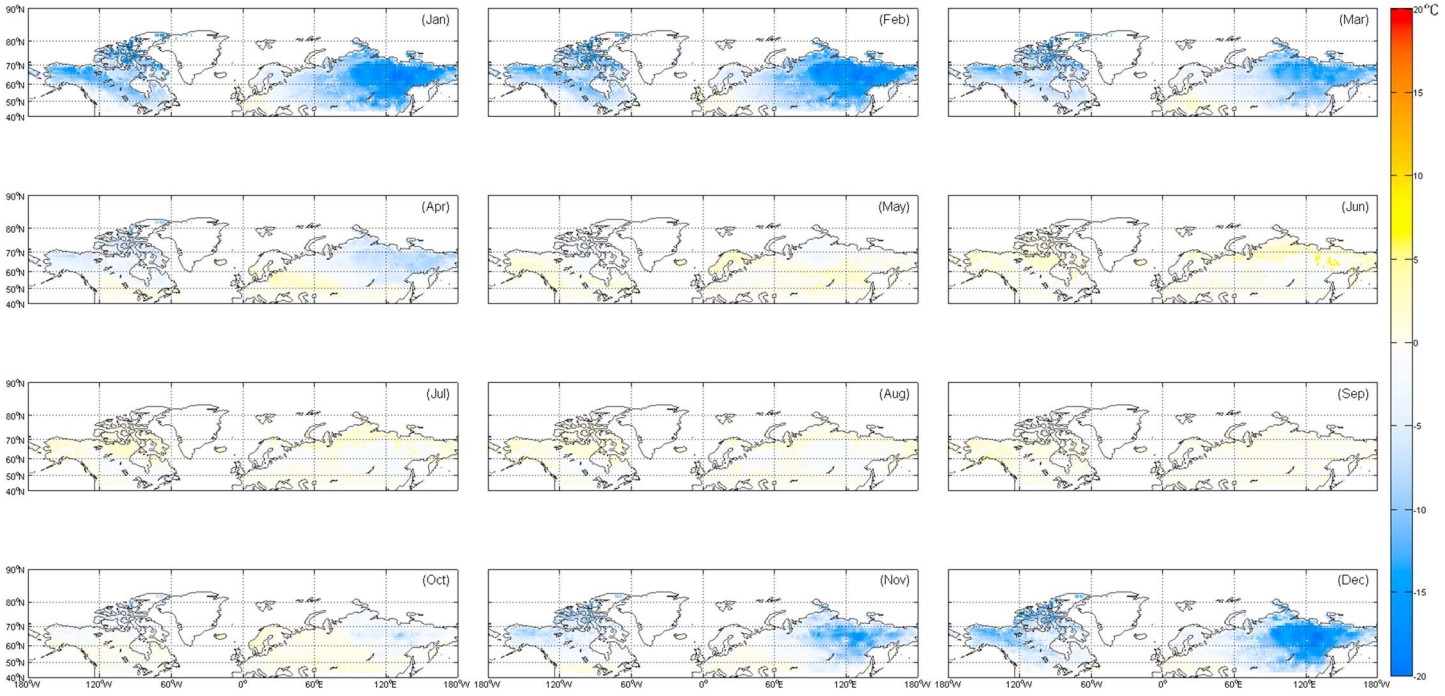

Figure 4. Spatial differences of monthly mean soil temperatures at 5-cm soil depth between the original model and the revised model.

gradually as the vertical depth increases. Although still warmer than the original estimation at 20 cm depth, the revised soil temperature estimation deviated less from the original one by 4.9°C in winter. This was also confirmed by the snow manipulation experiment data taken from surface down to 20 cm and even deeper (Hardy et al., 2001).

Soil temperature changes influenced ground freeze/thaw status (F/T), especially during the transitional seasons. F/T was assessed based on the near-surface soil temperature at 2 cm. Average −0.9°C was used as the freezing point to classify the ground F/T status (Kozlowski, 2004, 2009; Rivkina et al., 2000). The revised model estimated larger unfrozen ground area (0.9% to 2.4%) compared to the original model during May and November. Larger later spring unfrozen ground area was estimated over the Siberia and northwest Canada, and larger early winter unfrozen ground areas were mainly along the southern Canadian border and central to eastern Europe (Figure 5). These discrepancies were due to snow insulation effects.

The revised model estimated that permafrost area in July of 2010 was approximately 19.9×10^6 km^2, in which the active layer depth was shallower than 3 m. When the revised model was run to the end of 2099 under RCP2.6 and RCP8.5 scenarios, permafrost areas in July were estimated to shrink to 12.3×10^6 and 9.7×10^6 km^2, respectively. These projected permafrost areas were comparable with the estimates of 10.0×10^6 and 2.1×10^6 km^2 for RCP2.6 and RCP8.5, respectively, by Slater and Lawrence (2013) and within $5 \times 10^6 - 17 \times 10^6$ km^2 for RCP8.5 by Koven et al. (2015).

3.3. Snow Effects on Carbon Dynamics

3.3.1. Seasonal Carbon Dynamics

By explicitly considering the snow insulation effects, the revised model estimated higher soil respiration compared to the original model estimation (Figure 6b). During the coldest months, the revised model estimated 81.9 TgC/month more soil respiration on average (Figure 6b). This led to 458.0 Tg more soil C released during each nongrowing season (Figure 7a) if January to March and November to December was defined as nongrowing season in the region. During these months, monthly regional NEP of two versions deviated by 91.6 TgC (Figure 6c). As soil warming slows transitioning from winter to summer, the revised model estimates smaller spring GPP and negative NEP. Comparison between two estimations confirmed that the most significant seasonal NEP differences occurred in April and May, with 861.7 Tg less C accumulation each spring (Figures 6c and 7c) while the soil respiration was close to the original (16.6 Tg more C). GPP estimated

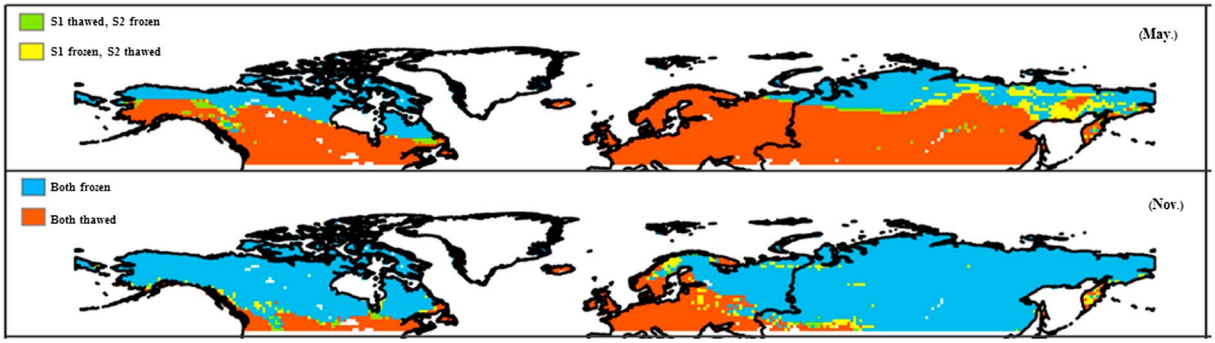

Figure 5. Freeze/thaw status in two transitional months of 2007 estimated with the original model (S1) and the revised model (S2).

from the revised model is similar to the original estimates after June, when there is no snow (Figure 6a). The revised model estimated 567.0 Tg less positive NEP. This is mainly due to slightly higher soil respiration induced by higher soil temperature (Figures 4 and 8). Two estimations during late fall season (September to October) were close, with 105.9 Tg less C lost each fall from the revised model on average (−87.4 TgC from the revised, compared to −193.4 TgC). The temporal pattern of monthly NEP agreed well with observations of Euskirchen et al. (2017), as well as the ensemble model simulations by McGuire et al. (2012) and Fisher et al. (2014), yet the detailed magnitude of which varied widely.

3.3.2. Interannual Variability of Carbon Dynamics

Monthly and seasonal deviations of the revised model from the previous estimation accumulated during 2003–2010, leading to nearly 0.7 Pg/year more soil C respired and 1.6 Pg/year less C sequestered to the ecosystem. Cumulative NEP differences between the two simulations by the end of the historical period

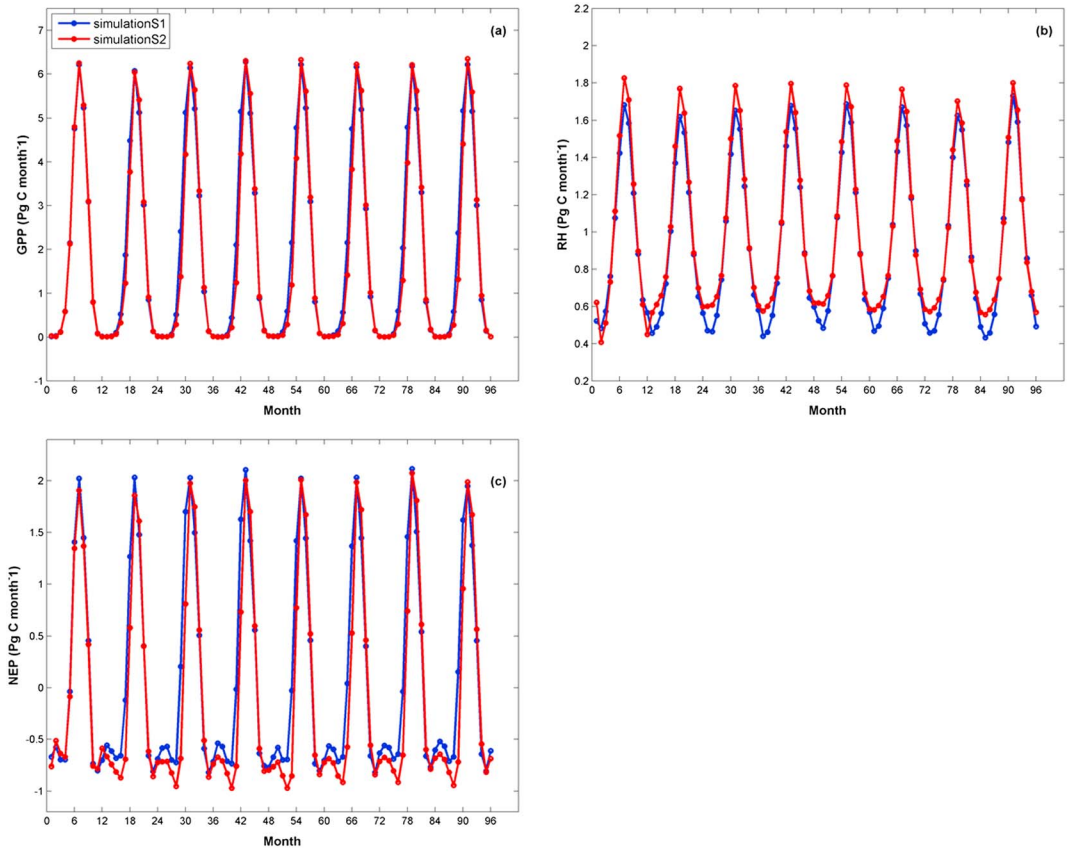

Figure 6. Monthly regional carbon fluxes over 2003–2010 estimated from two versions of the model: (a) gross primary production (GPP), (b) heterotrophic respiration (R_H), and (c) net ecosystem production (NEP).

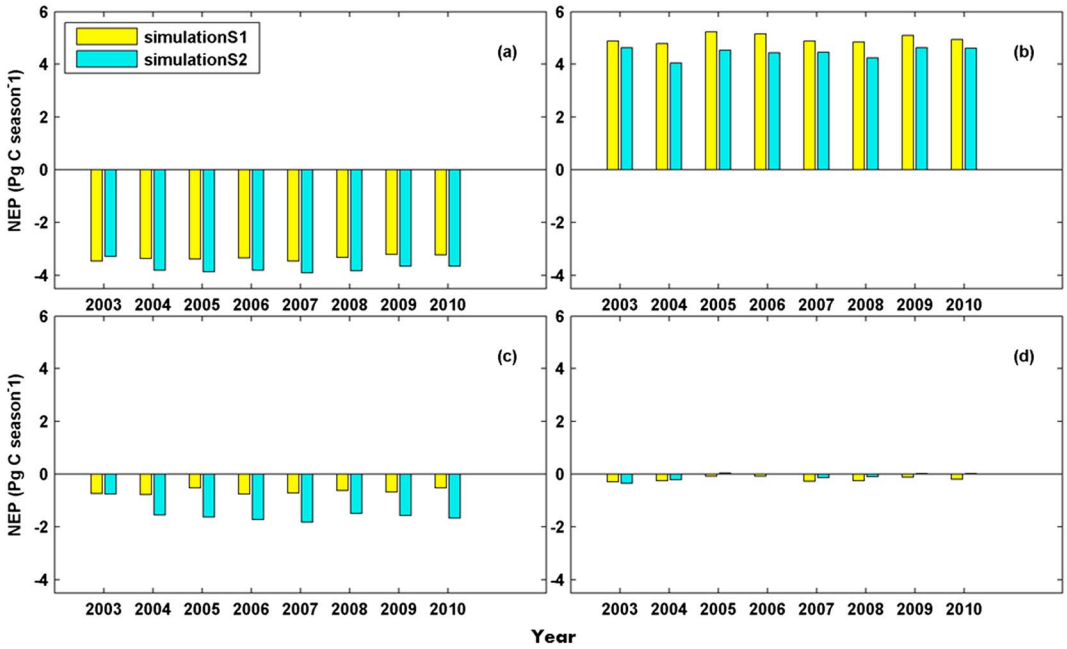

Figure 7. Regional net ecosystem production (NEP) for different seasons over 2003–2010 estimated with two versions of the model: (a) Nongrowing season (November–March); (b) growing season (June–August); (c) transitional spring season (April–May); and (d) transitional fall season (September–October).

amounted to 3.3 PgC (Figures 9 and 10). The original model estimated that the study area was a carbon sink at 768.6 TgC/year (Figure 9), while the revised model, by explicitly considering snow thickness and thermal conductivity, estimated a carbon source at −894.9 TgC/year (Figure 9). Spatial discrepancies between two NEP simulations were more evident in the region from southern Alaska and southern Canada, as well as in east Europe and Siberia (Figure 10). Specifically, Alaska was estimated as a C sink from 4.5 to 198.3 TgC/year during 2003–2010. On average, the revised estimation of annual NEP in Alaska was 66.6 TgC/year

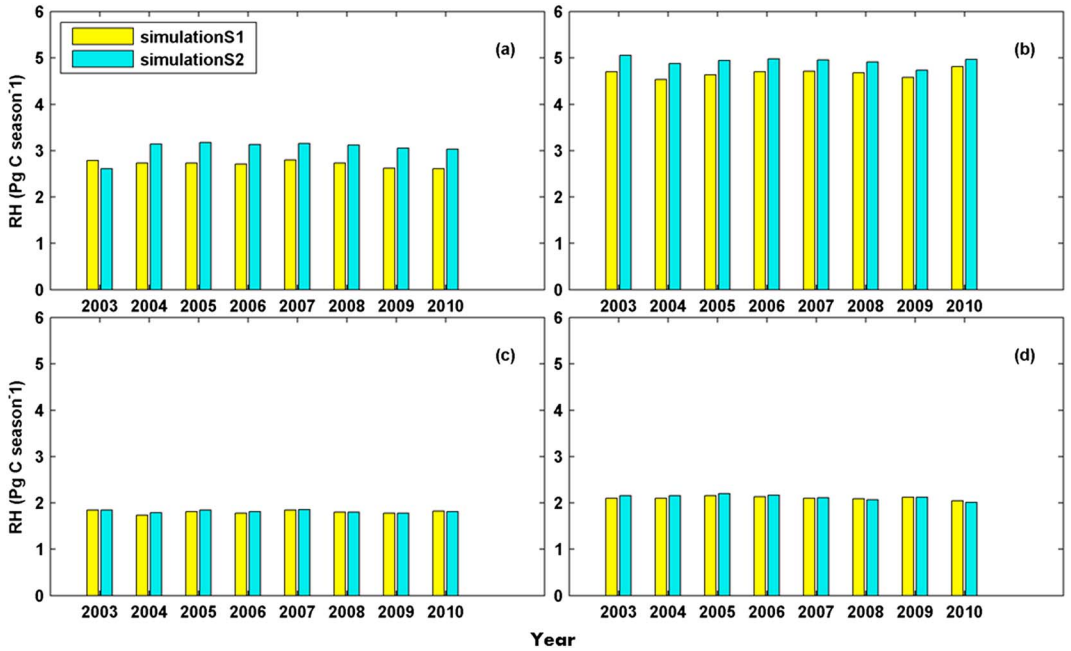

Figure 8. Regional heterotrophic respiration (R_H) for different seasons over 2003–2010 estimated with two versions of the model: (a) Nongrowing season (November–March); (b) growing season (June–August); (c) transitional spring season (April–May); and (d) transitional fall season (September–October).

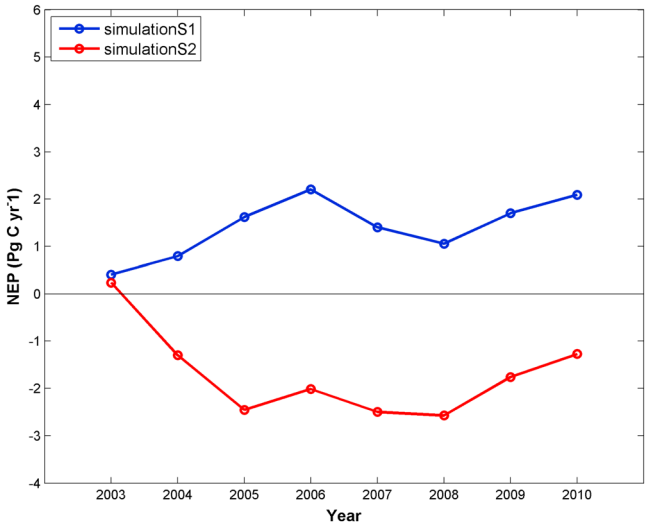

Figure 9. Cumulative regional annual net ecosystem production (NEP) over 2003–2010 from two versions of the model.

(−0.048 kgC/m^2/year), which was generally consistent with the multimodel mean NEP estimation of 0.01 ± 0.19 kgC/m^2/year by Fisher et al. (2014), and the much narrower range from McGuire et al. (2012) between a sink of 297 TgC/year and a source of −80 TgC/year for the entire Arctic. The original TEM estimated that the Arctic stored 722 PgC in soils (excluding Greenland) in comparison to 716 PgC simulated with the revised model at the end of 2010 (Figure 11). Differences between the two simulations were small, yet considering the relatively short period of time, this loss rate can be significant in the long run.

At the end of the projection period of 2017–2099 under RCP2.6 and RCP8.5 scenarios, soil C stocks (excluding Greenland) were estimated to be between 591.2 and 614.6 PgC, respectively (Figure 12). Warmer climate will likely enhance soil respiration, leading to a decrease in regional soil C stocks in the first half of the 21st century under both climate scenarios. Under the low CO_2 emission scenario (RCP2.6), soil C stocks will likely be steady in the latter half of the century. This agrees with several studies which indicate that the soil carbon loss more than offsets the increase of plant productivity due to CO_2 fertilization effects (Mack et al., 2004; Natali et al., 2014; Schaefer et al., 2011). However, the continued warming and increasing atmospheric CO_2 under the highest CO_2 emission scenario (RCP8.5) may transition the region into a weak carbon sink, with roughly an increase of 18 Pg soil C from the early 2060s to the end of 2099 (Figure 12). This transitional trend into a C sink under the high warming scenario in the 21st century was mainly due to greater plant productivity that overwhelmed the elevated soil decomposition, which was comparable to previous studies of McGuire et al. (2000) and Qian et al. (2010).

There are a few limitations to this study. First, the inherent nature of monthly step STM-TEM limited the model to quantify fine-scale (e.g., daily or diurnal) temporal thermal variation and evolution that affects ecosystem C cycling. Further, we have kept snow and soil thermal conductivity as well as snow density constant for each ecosystem over time, which will also bias the simulated soil thermal and C dynamics. Finer temporal resolution models will be more capable of addressing detailed processes and feedbacks such as the effects of snow density and thermal conductivity changes over time (Bormann et al., 2013; De Michele et al., 2013). Recent studies on nonlinear snow thermal conductance and heat fluxes by Jafarov et al. (2014) and Slater et al. (2017) could help our model development in this regard. Second, the revised model was calibrated to a limited number of observation sites with some degrees of human disturbance for only typical vegetation and soil types in the Arctic. The calibration data sets were all obtained from North America that mostly included soil thermal records from topsoil layers only and for a relatively short temporal extent. With more data becoming available such as described in Boike et al. (2013), and from Global Terrestrial Network for Permafrost, and U.S. Geological Survey sites, a more comprehensive study that utilizes various site-level climate and soil thermal records from undisturbed and less biased sites for all vegetation and soil types would help draw more robust conclusions. Third, all sites were calibrated using AMSR-E satellite SWE instead of in

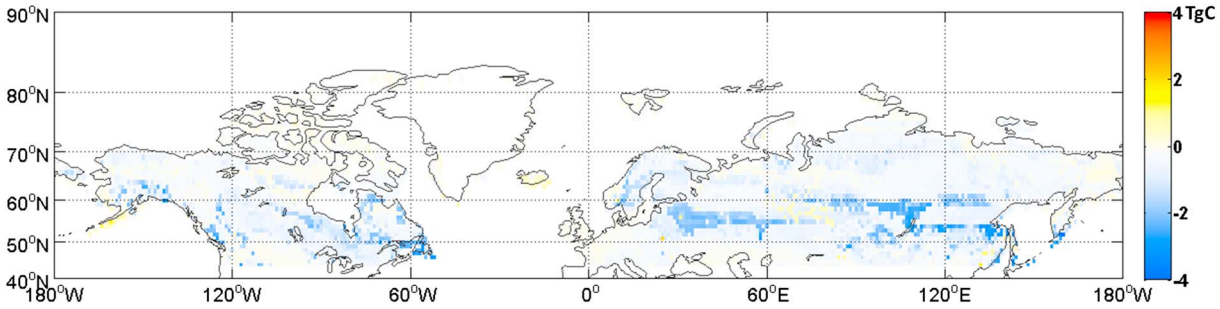

Figure 10. Simulated cumulative net ecosystem production differences between two versions of the model by the end of 2010.

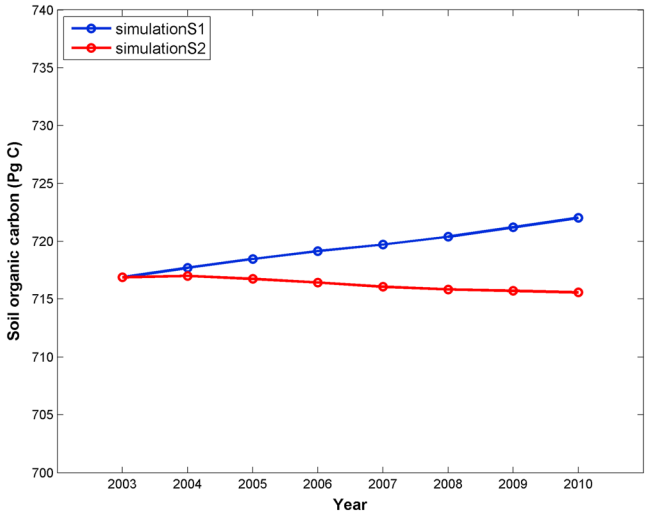

Figure 11. Estimated annual regional carbon over 2003–2010 from two versions of the model.

situ data due to data limitation. The spatial variability of snowpack due to topography, vegetation cover, and blowing wind leads to simulation errors when applied to site-level modeling. In order to quantify the influence of snow heterogeneity on soil thermal dynamics, a dynamic process-based snow model is needed (Broxton et al., 2015; Hiemstra et al., 2002, 2006). Further, unfrozen water has been indicated important in affecting winter soil respiration (Schaefer & Jafarov, 2016). Future model development could benefit from better soil moisture simulation in response to freeze-thaw dynamics. For instance, introducing scaling factors to model winter soil respiration affected by unfrozen water is necessary. Finally, we recognize that there might be biases using satellite observations (MEaSUREs Global Record of Daily Landscape Freeze/Thaw Status, Version 3, and Arctic Soil Freeze/Thaw Status from SMMR and SSM/I, Version 2, for instance) to characterize the landscape freeze/thaw status, because the data might have actually reflected canopy conditions rather than ground (Kim et al., 2011). Thus, more appropriate observational freeze/thaw data for model evaluation are also desirable.

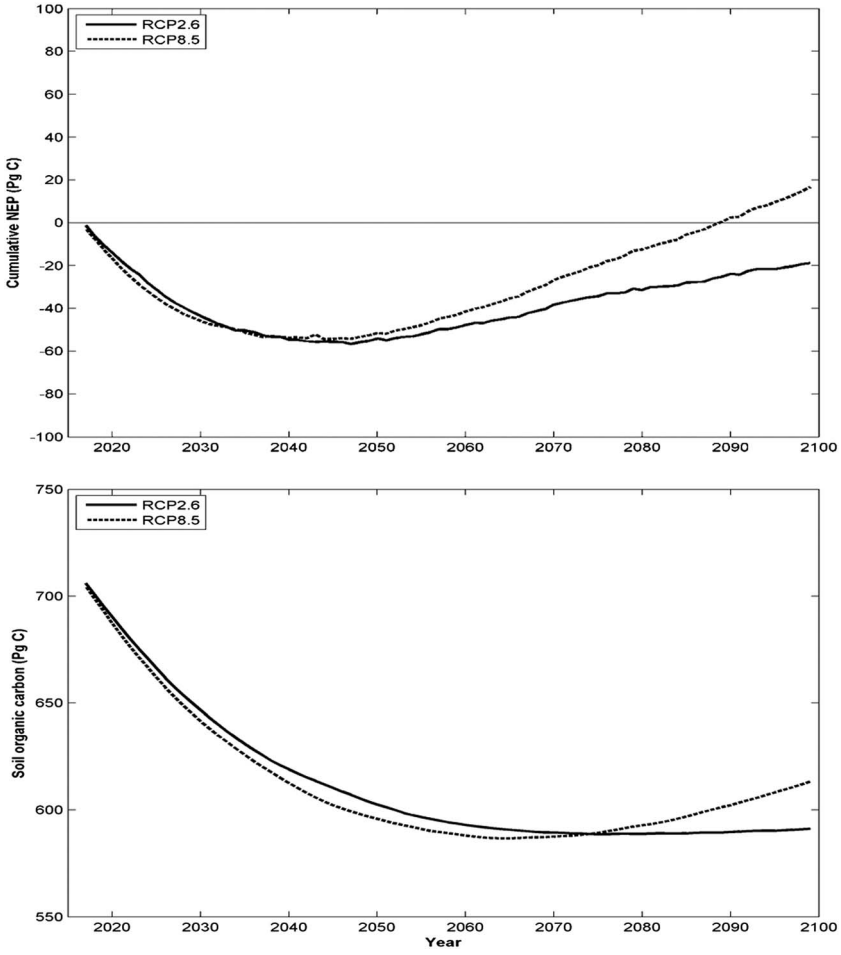

Figure 12. Projected net ecosystem production (NEP) (upper panel) and soil organic carbon (lower panel) in the Arctic from the revised model over 2017–2099, under Representative Concentration Pathway 2.6 (RCP2.6) and RCP8.5 scenarios.

4. Conclusions

Considering varying snow thickness and thermal conductivity, our revised model was more capable of estimating topsoil temperature profile in the Arctic. In the historical period, the revised model estimated 6.4°C warmer soil in nongrowing season, and a slower soil temperature transition in early spring and late fall, compared to the original model. The presence of snow also influenced ground freeze/thaw status. The frozen front estimated by the revised model during the historical period lay slightly northward over eastern Siberia in May, and in central to east Europe and along southern Canada in November. This study highlighted the prominent role of snow cover in the C cycling of northern ecosystems. On average, near 0.41 Pg more soil C was respired in each nongrowing season during 2003–2010 in the revised simulation due to snow insulation effects. Slower soil temperature transition in spring limits CO_2 uptake by plants, reducing GPP, and ultimately reducing seasonal sink by 0.86 PgC. Overall, the northern 45°–90°N region was a C source at 0.89 PgC/year during the historical period according to the revised simulation, opposed to a C sink at 0.77 PgC/year. Historical regional soil organic C stocks decreased by 0.19 PgC/year. Future projections under the low-emission scenario will likely stay as a carbon source. However, future projection under the high-emission scenario indicated that the region may gradually transition from a source into a weak sink in the latter half of the 21st century due to high plant productivity.

Acknowledgments

This research was supported by a NSF project (IIS-1027955), a DOE project (DE-SC0008092), and a NASA LCLUC project (NNX09AI26G) to Q. Z. We acknowledge the Rosen High Performance Computing Center at Purdue for computing support. We thank the National Snow and Ice Data center for providing Global Monthly EASE-Grid Snow Water Equivalent data, National Oceanic and Atmospheric Administration for North American Regional Reanalysis (NARR), and Hugelius and his group by making available pan-Arctic permafrost soil C maps. We also acknowledge the World Climate Research Programme's Working Group on Coupled Modeling Intercomparison Project CMIP5, and we thank the climate modeling groups for producing and making available their model output. The data presented in this paper can be accessed through our research website (http://www.eaps.purdue.edu/ebdl/).

References

Armstrong, R. L., & Brodzik, M. J. (2002). Hemispheric-scale comparison and evaluation of passive-microwave snow algorithms. *Annals of Glaciology*, *34*(1), 38–44. https://doi.org/10.3189/172756402781817428

Armstrong, R. L., Brodzik, M. J., Knowles, K., & Savoie, M. (2005). *Global monthly EASE-Grid snow water equivalent climatology. [2003 to 2010]*. Boulder, CO: NASA National Snow and Ice Data Center Distributed Active Archive Center. https://doi.org/10.5067/KJVERY3MIBPS

Baek, H. J., Lee, J., Lee, H. S., Hyun, Y. K., Cho, C., Kwon, W. T., et al. (2013). Climate change in the 21st century simulated by HadGEM2-AO under representative concentration pathways. *Asia-Pacific Journal of Atmospheric Sciences*, *49*(5), 603–618. https://doi.org/10.1007/s13143-013-0053-7

Batjes, N. H. (1996). Total carbon and nitrogen in the soils of the world. *European Journal of Soil Science*, *47*(2), 151–163. https://doi.org/10.1111/j.1365-2389.1996.tb01386.x

Belshe, E. F., Schuur, E. A. G., & Bolker, B. M. (2013). Tundra ecosystems observed to be CO_2 sources due to differential amplification of the carbon cycle. *Ecology Letters*, *16*(10), 1307–1315. https://doi.org/10.1111/ele.12164

Björkman, M. P., Morgner, E., Cooper, E. J., Elberling, B., Klemedtsson, L., & Björk, R. G. (2010). Winter carbon dioxide effluxes from Arctic ecosystems: An overview and comparison of methodologies. *Global Biogeochemical Cycles*, *24*, GB3010. https://doi.org/10.1029/2009GB003667

Boike, J., Kattenstroth, B., Abramova, K., Bornemann, N., Chetverova, A., Fedorova, I., Fröb, K., et al. (2013). Baseline characteristics of climate, permafrost, and land cover from Samoylov Island, Lena River Delta, Siberia.

Bond-Lamberty, B., Wang, C., & Gower, S. T. (2005). Spatiotemporal measurement and modeling of stand-level boreal forest soil temperatures. *Agricultural and Forest Meteorology*, *131*(1-2), 27–40. https://doi.org/10.1016/j.agrformet.2005.04.008

Bormann, K. J., Westra, S., Evans, J. P., & McCabe, M. F. (2013). Spatial and temporal variability in seasonal snow density. *Journal of Hydrology*, *484*, 63–73. https://doi.org/10.1016/j.jhydrol.2013.01.032

Brady, N. C., & Weil, R. (2013). In P. Higher (Ed.), *Nature and properties of soils, the: Pearson new international edition*. London, UK: Pearson Higher Ed.

Broxton, P. D., Harpold, A. A., Biederman, J. A., Troch, P. A., Molotch, N. P., & Brooks, P. D. (2015). Quantifying the effects of vegetation structure on snow accumulation and ablation in mixed-conifer forests. *Ecohydrology*, *8*(6), 1073–1094. https://doi.org/10.1002/eco.1565

Bulygina, O. N., Razuvaev, V. N., & Korshunova, N. N. (2009). Changes in snow cover over Northern Eurasia in the last few decades. *Environmental Research Letters*, *4*(4), 045026. https://doi.org/10.1088/1748-9326/4/4/045026

Chang, A. T. C., Foster, J. L., & Hall, D. K. (1987). Nimbus-7 SMMR derived global snow cover parameters. *Annals of Glaciology*, *9*, 39–44. https://doi.org/10.1017/S0260305500000355

Cherkauer, K. A., & Lettenmaier, D. P. (1999). Hydrologic effects of frozen soils in the upper Mississippi River basin. *Journal of Geophysical Research*, *104*(D16), 19,599–19,610. https://doi.org/10.1029/1999JD900337

De Michele, C., Avanzi, F., Ghezzi, A., & Jommi, C. (2013). Investigating the dynamics of bulk snow density in dry and wet conditions using a one-dimensional model. *The Cryosphere*, *7*(2), 433–444. https://doi.org/10.5194/tc-7-433-2013

Déry, S. J., & Brown, R. D. (2007). Recent Northern Hemisphere snow cover extent trends and implications for the snow-albedo feedback. *Geophysical Research Letters*, *34*, L22504. https://doi.org/10.1029/2007GL031474

Desai, A. R., Bolstad, P. V., Cook, B. D., Davis, K. J., & Carey, E. V. (2005). Comparing net ecosystem exchange of carbon dioxide between an old-growth and mature forest in the upper Midwest, USA. *Agricultural and Forest Meteorology*, *128*(1-2), 33–55. https://doi.org/10.1016/j.agrformet.2004.09.005

Dyer, J. L., & Mote, T. L. (2006). Spatial variability and trends in observed snow depth over North America. *Geophysical Research Letters*, *33*, L16503. https://doi.org/10.1029/2006GL027258

Edenhofer, O., Pichs-Madruga, R., Sokona, Y., Farahani, E., Kadner, S., Seyboth, K., et al. (2014). Climate change 2014: Mitigation of climate change. In *Contribution of Working Group III to the Fifth Assessment Report of the Intergovernmental Panel on Climate Change* (pp. 511–597). Cambridge, UK: Cambridge University Press.

Euskirchen, E. S., Bret-Harte, M. S., Scott, G. J., Edgar, C., & Shaver, G. R. (2012). Seasonal patterns of carbon dioxide and water fluxes in three representative tundra ecosystems in northern Alaska. *Ecosphere*, *3*(1), 1–19.

Euskirchen, E. S., Bret-Harte, M. S., Shaver, G. R., Edgar, C. W., & Romanovsky, V. E. (2017). Long-term release of carbon dioxide from arctic tundra ecosystems in Alaska. *Ecosystems*, *20*(5), 960–974.

Fierer, N., Schimel, J. P., & Holden, P. A. (2003). Variations in microbial community composition through two soil depth profiles. *Soil Biology and Biochemistry*, *35*(1), 167–176. https://doi.org/10.1016/S0038-0717(02)00251-1

Fisher, J. B., Sikka, M., Oechel, W. C., Huntzinger, D. N., Melton, J. R., Koven, C. D., et al. (2014). Carbon cycle uncertainty in the Alaskan Arctic. *Biogeosciences*, *11*(15), 4271–4288. https://doi.org/10.5194/bg-11-4271-2014

Fisk, M. C., Ruether, K. F., & Yavitt, J. B. (2003). Microbial activity and functional composition among northern peatland ecosystems. *Soil Biology and Biochemistry*, *35*(4), 591–602. https://doi.org/10.1016/S0038-0717(03)00053-1

Food and Agriculture Organization (1974). *Soil map of the world* (Vol. I-X). Paris, France: United Nations Educational, Scientific and Cultural Organization.

Grogan, P. (2012). Cold season respiration across a low arctic landscape: The influence of vegetation type, snow depth, and interannual climatic variation. *Arctic, Antarctic, and Alpine Research*, *44*(4), 446–456. https://doi.org/10.1657/1938-4246-44.4.446

Hardy, J. P., Groffman, P. M., Fitzhugh, R. D., Henry, K. S., Welman, A. T., Demers, J. D., et al. (2001). Snow depth manipulation and its influence on soil frost and water dynamics in a northern hardwood forest. *Biogeochemistry*, *56*(2), 151–174. https://doi.org/10.1023/A:1013036803050

Hayes, D. J., McGuire, A. D., Kicklighter, D. W., Gurney, K. R., Burnside, T. J., & Melillo, J. M. (2011). Is the northern high-latitude land-based CO_2 sink weakening? *Global Biogeochemical Cycles*, *25*, GB3018. https://doi.org/10.1029/2010GB003813

Hiemstra, C. A., Liston, G. E., & Reiners, W. A. (2002). Snow redistribution by wind and interactions with vegetation at upper treeline in the Medicine Bow Mountains, Wyoming, USA. *Arctic, Antarctic, and Alpine Research*, *34*(3), 262–273. https://doi.org/10.2307/1552483

Hiemstra, C. A., Liston, G. E., & Reiners, W. A. (2006). Observing, modelling, and validating snow redistribution by wind in a Wyoming upper treeline landscape. *Ecological Modelling*, *197*(1–2), 35–51. https://doi.org/10.1016/j.ecolmodel.2006.03.005

Hollinger, D. Y., Goltz, S. M., Davidson, E. A., Lee, J. T., Tu, K., & Valentine, H. T. (1999). Seasonal patterns and environmental control of carbon dioxide and water vapour exchange in an ecotonal boreal forest. *Global Change Biology*, *5*(8), 891–902. https://doi.org/10.1046/j.1365-2486.1999.00281.x

Hugelius, G., Strauss, J., Zubrzycki, S., Harden, J. W., Schuur, E., Ping, C. L., et al. (2014). Estimated stocks of circumpolar permafrost carbon with quantified uncertainty ranges and identified data gaps. *Biogeosciences*, *11*(23), 6573–6593. https://doi.org/10.5194/bg-11-6573-2014

Hugelius, G., Tarnocai, C., Broll, G., Canadell, J. G., Kuhry, P., & Swanson, D. K. (2013). The northern circumpolar soil carbon database: Spatially distributed datasets of soil coverage and soil carbon storage in the northern permafrost regions. *Earth System Science Data*, *5*(1), 3–13. https://doi.org/10.5194/essd-5-3-2013

Ikawa, H., & Oechel, W. C. (2014). Spatial and temporal variability of air-sea CO_2 exchange of alongshore waters in summer near Barrow, Alaska. *Estuarine, Coastal and Shelf Science*, *141*, 37–46. https://doi.org/10.1016/j.ecss.2014.02.002

Iman, R. L. (2008). Latin hypercube sampling. In *Encyclopedia of quantitative risk analysis and assessment* (pp. 1–5). https://doi.org/10.1002/9780470061596.risk0299

Intergovernmental Panel on Climate Change (2014). *Climate change 2014–Impacts, adaptation and vulnerability: Regional aspects*. Cambridge, UK: Cambridge University Press.

Jafarov, E. E., Nicolsky, D. J., Romanovsky, V. E., Walsh, J. E., Panda, S. K., & Serreze, M. C. (2014). The effect of snow: How to better model ground surface temperatures. *Cold Regions Science and Technology*, *102*, 63–77. https://doi.org/10.1016/j.coldregions.2014.02.007

Jobbágy, E. G., & Jackson, R. B. (2000). The vertical distribution of soil organic carbon and its relation to climate and vegetation. *Ecological Applications*, *10*(2), 423–436. https://doi.org/10.1890/1051-0761(2000)010%5B0423:TVDOSO%5D2.0.CO;2

Kim, Y., Kimball, J. S., McDonald, K. C., & Glassy, J. (2011). Developing a global data record of daily landscape freeze/thaw status using satellite passive microwave remote sensing. *IEEE Transactions on Geoscience and Remote Sensing*, *49*(3), 949–960. https://doi.org/10.1109/TGRS.2010.2070515

Koven, C. D., Schuur, E. A. G., Schädel, C., Bohn, T. J., Burke, E. J., Chen, G., et al. (2015). A simplified, data-constrained approach to estimate the permafrost carbon–climate feedback. *Philosophical Transactions of the Royal Society A*, *373*(2054), 20140423. https://doi.org/10.1098/rsta.2014.0423

Kozlowski, T. (2004). Soil freezing point as obtained on melting. *Cold Regions Science and Technology*, *38*(2-3), 93–101. https://doi.org/10.1016/j.coldregions.2003.09.001

Kozlowski, T. (2009). Some factors affecting supercooling and the equilibrium freezing point in soil–water systems. *Cold Regions Science and Technology*, *59*(1), 25–33. https://doi.org/10.1016/j.coldregions.2009.05.009

Kwon, H. J., Oechel, W. C., Zulueta, R. C., & Hastings, S. J. (2006). Effects of climate variability on carbon sequestration among adjacent wet sedge tundra and moist tussock tundra ecosystems. *Journal of Geophysical Research*, *111*, G03014. https://doi.org/10.1029/2005JG000036

Lawrence, D. M., & Slater, A. G. (2010). The contribution of snow condition trends to future ground climate. *Climate Dynamics*, *34*(7–8), 969–981. https://doi.org/10.1007/s00382-009-0537-4

Lemke, P., Ren, J., Alley, R. B., Allison, I., Carrasco, J., Flato, G., et al. (2007). Observations: Changes in snow, ice and frozen ground.

Mack, M. C., Schuur, E. A., Bret-Harte, M. S., Shaver, G. R., & Chapin, F. S. III (2004). Ecosystem carbon storage in arctic tundra reduced by long-term nutrient fertilization. *Nature*, *431*(7007), 440–443. https://doi.org/10.1038/nature02887

Martin, G. M., Bellouin, N., Collins, W. J., Culverwell, I. D., Halloran, P. R., Hardiman, S. C., et al. (2011). The HadGEM2 family of Met Office Unified Model climate configurations. *Geoscientific Model Development*, *4*, 723–757.

McCarthy, J. J. (2001). *Climate change 2001: Impacts, adaptation, and vulnerability: Contribution of Working Group II to the third assessment report of the Intergovernmental Panel on Climate Change*. Cambridge, UK: Cambridge University Press.

McCaughey, J. H., Lafleur, P. M., Joiner, D. W., Bartlett, P. A., Costello, A. M., Jelinski, D. E., & Ryan, M. G. (1997). Magnitudes and seasonal patterns of energy, water, and carbon exchanges at a boreal young jack pine forest in the BOREAS northern study area. *Journal of Geophysical Research*, *102*(D24), 28,997–29,007. https://doi.org/10.1029/97JD00239

McGuire, A. D., Christensen, T. R., Hayes, D., Heroult, A., Euskirchen, E., Kimball, J. S., et al. (2012). An assessment of the carbon balance of Arctic tundra: Comparisons among observations, process models, and atmospheric inversions. *Biogeosciences*, *9*(8), 3185–3204. https://doi.org/10.5194/bg-9-3185-2012

McGuire, A. D., Clein, J. S., Melillo, J. M., Kicklighter, D. W., Meier, R. A., Vorosmarty, C. J., & Serreze, M. C. (2000). Modelling carbon responses of tundra ecosystems to historical and projected climate: Sensitivity of pan-Arctic carbon storage to temporal and spatial variation in climate. *Global Change Biology*, *6*(S1), 141–159. https://doi.org/10.1046/j.1365-2486.2000.06017.x

McGuire, A. D., Koven, C., Lawrence, D. M., Clein, J. S., Xia, J., Beer, C., et al. (2016). Variability in the sensitivity among model simulations of permafrost and carbon dynamics in the permafrost region between 1960 and 2009. *Global Biogeochemical Cycles*, *30*(7), 1015–1037. https://doi.org/10.1002/2016GB005405

Melillo, J. M., McGuire, A. D., Kicklighter, D. W., Moore, B., Vorosmarty, C. J., & Schloss, A. L. (1993). Global climate change and terrestrial net primary production. *Nature*, *363*(6426), 234–240. https://doi.org/10.1038/363234a0

Mitchell, T. D., Carter, T. R., Jones, P. D., Hulme, M., & New, M. (2004). A comprehensive set of high-resolution grids of monthly climate for Europe and the globe: The observed record (1901–2000) and 16 scenarios (2001–2100). *Tyndall Centre for Climate Change Research Working Paper*, *55*, 25.

Natali, S. M., Schuur, E. A., Webb, E. E., Pries, C. E. H., & Crummer, K. G. (2014). Permafrost degradation stimulates carbon loss from experimentally warmed tundra. *Ecology*, *95*(3), 602–608. https://doi.org/10.1890/13-0602.1

NCAR/NAVY (1984). *Global 10-minute elevation data*. Boulder, CO: National Geophysical Data Center.

Oberbauer, S. F., Tweedie, C. E., Welker, J. M., Fahnestock, J. T., Henry, G. H., Webber, P. J., et al. (2007). Tundra CO_2 fluxes in response to experimental warming across latitudinal and moisture gradients. *Ecological Monographs*, *77*(2), 221–238. https://doi.org/10.1890/06-0649

Oechel, W. C., Laskowski, C. A., Burba, G., Gioli, B., & Kalhori, A. A. (2014). Annual patterns and budget of CO_2 flux in an Arctic tussock tundra ecosystem. *Journal of Geophysical Research: Biogeosciences*, *119*(3), 323–339. https://doi.org/10.1002/2013JG002431

Osterkamp, T. E. (2007). Characteristics of the recent warming of permafrost in Alaska. *Journal of Geophysical Research*, *112*, F02S02. https://doi.org/10.1029/2006JF000578

Osterkamp, T. E., & Romanovsky, V. E. (1999). Evidence for warming and thawing of discontinuous permafrost in Alaska. *Permafrost and Periglacial Processes*, *10*(1), 17–37. https://doi.org/10.1002/(SICI)1099-1530(199901/03)10:1%3C17::AID-PPP303%3E3.0.CO;2-4

Qian, H., Joseph, R., & Zeng, N. (2010). Enhanced terrestrial carbon uptake in the northern high latitudes in the 21st century from the coupled carbon cycle climate model intercomparison project model projections. *Global Change Biology*, *16*(2), 641–656. https://doi.org/10.1111/j.1365-2486.2009.01989.x

Riedel, S. M., Epstein, H. E., Walker, D. A., Richardson, D. L., Calef, M. P., Edwards, E., & Moody, A. (2005). Spatial and temporal heterogeneity of vegetation properties among four tundra plant communities at Ivotuk, Alaska, USA. *Arctic, Antarctic, and Alpine Research*, *37*(1), 25–33. https://doi.org/10.1657/1523-0430(2005)037%5B0025:SATHOV%5D2.0.CO;2

Rivkina, E. M., Friedmann, E. I., McKay, C. P., & Gilichinsky, D. A. (2000). Metabolic activity of permafrost bacteria below the freezing point. *Applied and Environmental Microbiology*, *66*(8), 3230–3233. https://doi.org/10.1128/AEM.66.8.3230-3233.2000

Schaefer, K., & Jafarov, E. (2016). A parameterization of respiration in frozen soils based on substrate availability. *Biogeosciences*, *13*(7), 1991–2001. https://doi.org/10.5194/bg-13-1991-2016

Schaefer, K., Zhang, T. J., Bruhwiler, L., & Barrett, A. P. (2011). Amount and timing of permafrost carbon release in response to climate warming. *Tellus Series B: Chemical and Physical Meteorology*, *63*(2), 165–180. https://doi.org/10.1111/j.1600-0889.2011.00527.x

Schimel, J. P., Fahnestock, J., Michaelson, G., Mikan, C., Ping, C. L., Romanovsky, V. E., & Welker, J. (2006). Cold-season production of CO_2 in arctic soils: Can laboratory and field estimates be reconciled through a simple modeling approach? *Arctic, Antarctic, and Alpine Research*, *38*(2), 249–256. https://doi.org/10.1657/1523-0430(2006)38%5B249:CPOCIA%5D2.0.CO;2

Schindler, D. W., & Donahue, W. F. (2006). An impending water crisis in Canada's western prairie provinces. *Proceedings of the National Academy of Sciences of the United States of America*, *103*(19), 7210–7216. https://doi.org/10.1073/pnas.0601568103

Serreze, M. C., & Francis, J. A. (2006). The Arctic amplification debate. *Climatic Change*, *76*(3–4), 241–264. https://doi.org/10.1007/s10584-005-9017-y

Slater, A. G., & Lawrence, D. M. (2013). Diagnosing present and future permafrost from climate models. *Journal of Climate*, *26*(15), 5608–5623. https://doi.org/10.1175/JCLI-D-12-00341.1

Slater, A. G., Lawrence, D. M., & Koven, C. D. (2017). Process-level model evaluation: A snow and heat transfer metric. *The Cryosphere*, *11*(2), 989–996. https://doi.org/10.5194/tc-11-989-2017

Stieglitz, M., Déry, S. J., Romanovsky, V. E., & Osterkamp, T. E. (2003). The role of snow cover in the warming of arctic permafrost. *Geophysical Research Letters*, *30*(13), 1721. https://doi.org/10.1029/2003GL017337

Sturm, M., Holmgren, J., König, M., & Morris, K. (1997). The thermal conductivity of seasonal snow. *Journal of Glaciology*, *43*(143), 26–41. https://doi.org/10.1017/S0022143000002781

Sturm, M., Holmgren, J., & Liston, G. E. (1995). A seasonal snow cover classification system for local to global applications. *Journal of Climate*, *8*(5), 1261–1283. https://doi.org/10.1175/1520-0442(1995)008%3C1261:ASSCCS%3E2.0.CO;2

Sturm, M., Taras, B., Liston, G. E., Derksen, C., Jonas, T., & Lea, J. (2010). Estimating snow water equivalent using snow depth data and climate classes. *Journal of Hydrometeorology*, *11*(6), 1380–1394. https://doi.org/10.1175/2010JHM1202.1

Taylor, J. P., Wilson, B., Mills, M. S., & Burns, R. G. (2002). Comparison of microbial numbers and enzymatic activities in surface soils and subsoils using various techniques. *Soil Biology and Biochemistry*, *34*(3), 387–401. https://doi.org/10.1016/S0038-0717(01)00199-7

Taylor, K. E., Stouffer, R. J., & Meehl, G. A. (2012). An overview of CMIP5 and the experiment design. *Bulletin of the American Meteorological Society*, *93*(4), 485–498. https://doi.org/10.1175/BAMS-D-11-00094.1

Tian, H., Melillo, J. M., Kicklighter, D. W., McGuire, A. D., & Helfrich, J. V. K. I. (1999). The sensitivity of terrestrial carbon storage to historical climate variability and atmospheric CO_2 in the United States. *Tellus Series B: Chemical and Physical Meteorology*, *51*(2), 414–452. https://doi.org/10.3402/tellusb.v51i2.16318

Ueyama, M., Iwata, H., Harazono, Y., Euskirchen, E. S., Oechel, W. C., & Zona, D. (2013). Growing season and spatial variations of carbon fluxes of Arctic and boreal ecosystems in Alaska (USA). *Ecological Applications*, *23*(8), 1798–1816. https://doi.org/10.1890/11-0875.1

Valentini, R., Matteucci, G., Dolman, A. J., Schulze, E. D., Rebmann, C. J. M. E. A. G., Moors, E. J., et al. (2000). Respiration as the main determinant of carbon balance in European forests. *Nature*, *404*(6780), 861–865. https://doi.org/10.1038/35009084

Webb, E. E., Schuur, E. A., Natali, S. M., Oken, K. L., Bracho, R., Krapek, J. P., et al. (2016). Increased wintertime CO_2 loss as a result of sustained tundra warming. *Journal of Geophysical Research: Biogeosciences*, *121*, 249–265. https://doi.org/10.1002/2014JG002795

Zhang, T. (2005). Influence of the seasonal snow cover on the ground thermal regime: An overview. *Reviews of Geophysics*, *43*, RG4002. https://doi.org/10.1029/2004RG000157

Zhang, Y., Wang, S., Barr, A. G., & Black, T. A. (2008). Impact of snow cover on soil temperature and its simulation in a boreal aspen forest. *Cold Regions Science and Technology*, *52*(3), 355–370. https://doi.org/10.1016/j.coldregions.2007.07.001

Zhuang, Q., He, J., Lu, Y., Ji, L., Xiao, J., & Luo, T. (2010). Carbon dynamics of terrestrial ecosystems on the Tibetan Plateau during the 20th century: An analysis with a process-based biogeochemical model. *Global Ecology and Biogeography*, *19*(5), 649–662.

Zhuang, Q., McGuire, A. D., Melillo, J. M., Clein, J. S., Dargaville, R. J., Kicklighter, D. W., et al. (2003). Carbon cycling in extratropical terrestrial ecosystems of the Northern Hemisphere during the 20th century: A modeling analysis of the influences of soil thermal dynamics. *Tellus B*, *55*(3), 751–776. https://doi.org/10.1034/j.1600-0889.2003.00060.x

Zhuang, Q., Romanovsky, V. E., & McGuire, A. D. (2001). Incorporation of a permafrost model into a large-scale ecosystem model: Evaluation of temporal and spatial scaling issues in simulating soil thermal dynamics. *Journal of Geophysical Research*, *106*(D24), 33,649–33,670. https://doi.org/10.1029/2001JD900151

Zona, D., Gioli, B., Commane, R., Lindaas, J., Wofsy, S. C., Miller, C. E., et al. (2016). Cold season emissions dominate the Arctic tundra methane budget. *Proceedings of the National Academy of Sciences of the United States of America*, *113*(1), 40–45. https://doi.org/10.1073/pnas.1516017113